ENE 426 Final Report

Group D

Sining Niu

Marco Kleimans

Zijiao Zhang

Catherine Knox

# Contents

## *Introduction:*

Air pollution is a serious challenge in Los Angeles, as it results in decreased visibility, degradation to buildings, and respiratory health problems. In this assignment, we sought to characterize common characteristics of particulate air pollution using data from the city.

This report includes particulate statistics, design of a cascade impactor to collect particulates of various sizes, an analysis of respiratory deposition, analysis of optical properties, analysis of condensational growth under a variety of relative humidity and salt conditions, and the design of an electrostatic precipitator (ESP) to control particulate emissions from an industrial plant.

These results of these steps will allow policy makers and officials to build pertinent policies to limit air pollution in LA. It will also investigate the efficiency of an ESP to limit these particulates. This project can also be applied to the current Coronavirus pandemic, as section C will illustrate how the virus can be spread and directly enter the lungs of a patient.

## *Part A: Particle Statistics (Sining Niu and Catherine Knox)*

*Introduction:*

This particle size distribution data is retrieved from a real-world particle measurement in central Los Angeles. In part A, basic statistical analyses are conducted, and we could obtain a general interpretation of this data set.

*Calculations and results:*

First, particle number distribution could be calculated:

$$dN = \frac{dN}{dlogd_p} \times \Delta logd_p$$

Then, total surface and volume and mass concentration can be obtained:

$$Total\ surface\ concentration = \sum(\pi \times {d_p}^2 \times dN) = \mathbf{5.96 \times 10^8\ nm^2/cm^3}$$

$$Total\ volume\ concentration = \sum(\frac{\pi}{6} \times {d_p}^3 \times dN) = \mathbf{2.87 \times 10^{10}\ nm^3/cm^3}$$

$$Total\ mass\ concentration = \sum(\frac{\pi}{6} \times {d_p}^3 \times dN \times \rho) = \mathbf{2.88 \times 10^{-11}\ g/cm^3}$$

Average and median diameters were obtained as following:

$$Number\ based\ concentration\ average\ diameter = \frac{\sum(N_i d_i)}{N} = \mathbf{71.82nm}$$

$$Surface\ based\ concentration\ average\ diameter = (\frac{\sum N_i {d_i}^2}{N})^{1/2} = \mathbf{105nm}$$

$$Volume/Mass\ based\ concentration\ average\ diameter = (\frac{\sum N_i {d_i}^3}{N})^{1/3} = \mathbf{150nm}$$

Calculation of median diameter based on geometric mean:

$$Number\ based\ concentration\ median\ diameter = exp(\frac{\sum N_i ln(d_i)}{N}) = \mathbf{47.9nm}$$

$$Surface\ based\ concentration\ median\ diameter = exp(\frac{\sum S_i ln(d_i)}{S}) = \mathbf{214.3nm}$$

$$Volume/Mass\ based\ concentration\ median\ diameter = exp(\frac{\sum V_i ln(d_i)}{V}) = \mathbf{418.4nm}$$

Calculation of median diameter with 50% cumulation:

$$Number\ based\ concentration\ median\ diameter = \mathbf{41.4nm}$$

$$Surface\ based\ concentration\ median\ diameter = \mathbf{229.7nm}$$

$$Volume/Mass\ based\ concentration\ median\ diameter = \mathbf{346nm}$$

Geometric standard deviation:

$$GSD = \frac{d_{50}}{d_{15.78}}$$

$$Number\ based\ concentration\ GSD = d_{50}/d_{15.78} = 41.40/19.50 = \mathbf{2.12}$$

$$Surface\ based\ concentration\ GSD = d_{50}/d_{15.78} = 229.70/98.20 = \mathbf{2.34}$$

$$Volume/Mass\ based\ concentration\ GSD = d_{50}/d_{15.78} = 346.00/192 = \mathbf{1.80}$$

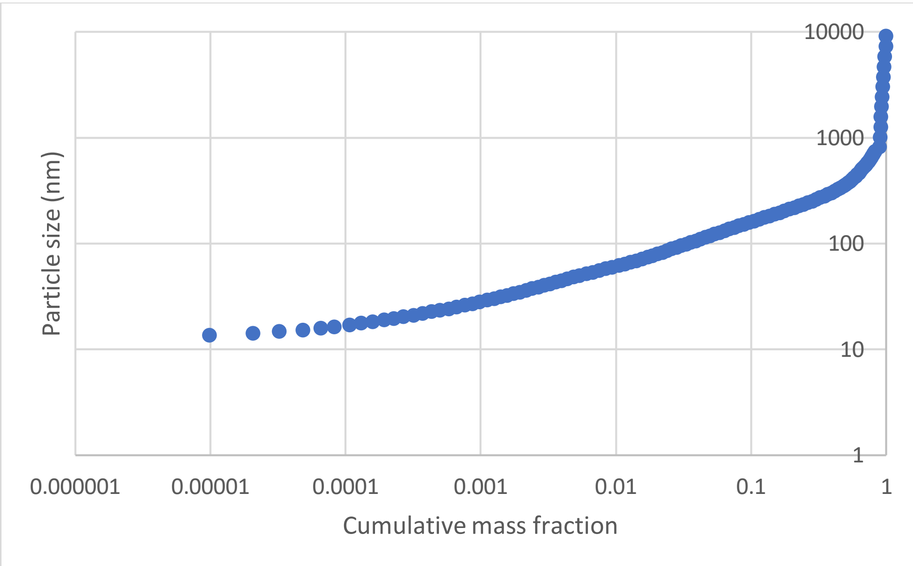


Figure A.1. Plot of particle size versus cumulative mass fraction in a log-log scale.

As we obtain the plot above, which is nearly a straight line, we can say that this data set is **lognormal distribution**.

**Deposition:**

t = 1 hr, A = 1m$^2$, λ = 66.7nm

$$C_C = 1 + 1.7 \times 2 \times \frac{\lambda}{d_p}$$

Diffusion deposition:

$$D = \frac{kTC_C}{3\pi\eta d}$$

$$N(t) = 2n_0(\frac{Dt}{\pi})^{0.5}A$$

Settling deposition:

$$V_{TS} = \frac{\rho_p d_p^2 g C_C}{18\mu}$$

$$N(t) = V_{TS} \times A \times t \times n_0$$

Calculation results are shown in the figures below:

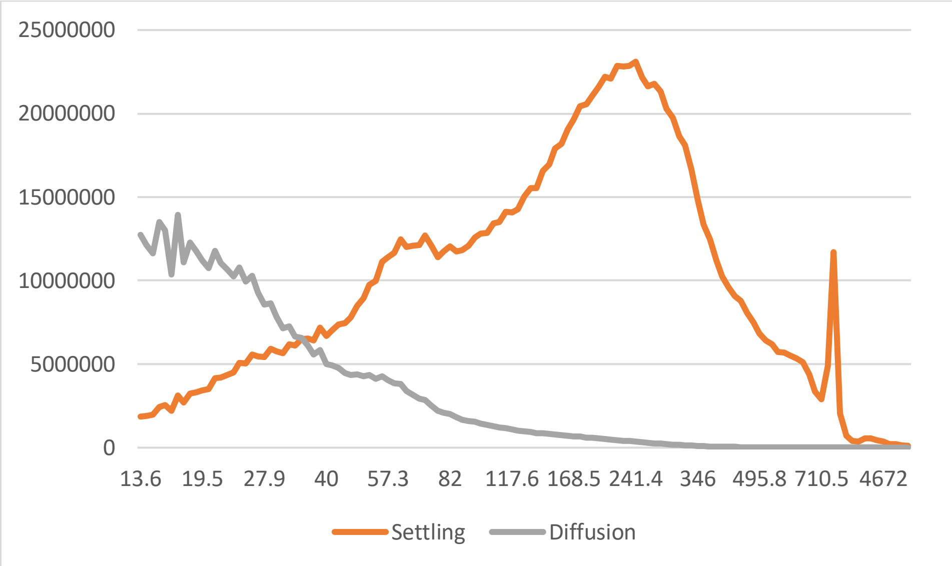


Figure A.2. Plot of settling and diffusion settling particle numbers at different particle size.

The outlier above for settling deposition around 800nm is due to a sudden increase of particle number concentration. This sudden increase might be the result of measure error.

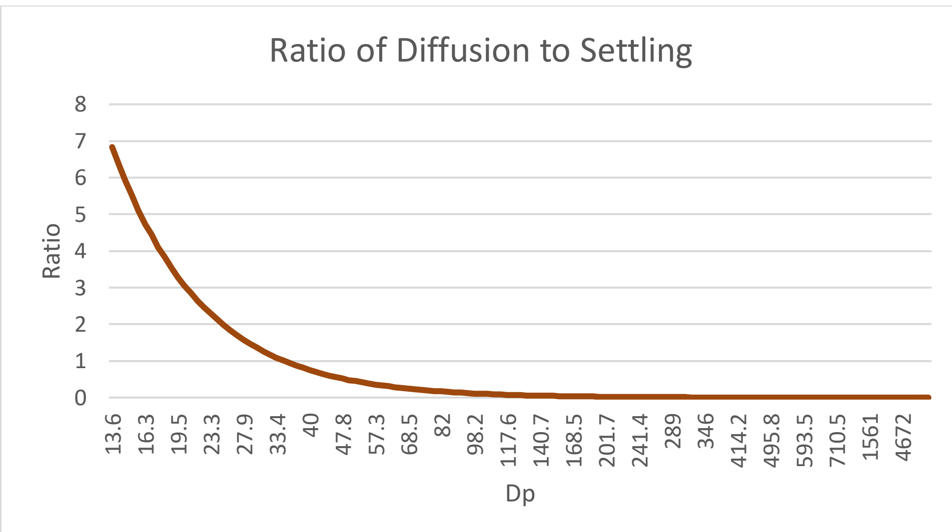


Figure A.3. Plot of the ratio of diffusion to settling deposition at a function of particle size.

As shown above in Figure A.3., the ratio of diffusion to settling deposition decreases as particle size increases. This is because the smaller particles have larger diffusivity and larger particles would prefer gravitational settling.

## *Part B: Cascade Impactor Design (Catherine Knox)*

*Introduction:*

In this section, we will design a cascade impactor to capture 200 ug of particulates in each stage. This allows for further analysis of the Los Angeles particulates.

*Calculations and Results:*

Mass concentrations were obtained from Part A and shown in the table below:

| Size | #Concentration/cm^3 | Mass concentration (g/cm^3) |
|---|---|---|
| <0.2 | 16364 | 4.78E-12 |
| 0.2-0.5 | 1172 | 1.47E-11 |
| 0.5-1 | 48.5 | 6.39E-12 |
| 1-2.5 | .89 | 9.66E-13 |
| 2.5-5 | .039 | 9.54E-13 |
| 5-10 | .005 | 7.42E-13 |

Table B.1. Mass concentrations for each selected bin size.

Based on these values, we design the impactor for the stage with the lowest mass concentration, given by 5-10 um at $7.42 * 10^{-13}\ g/cm^3$. Additionally, we know that the sampling period is 2 days and the required sample is 200 ug. Flow can be calculated as shown below:

$$sample\ required = 200\ ug$$
$$sampling\ period = 2\ days$$
$$Mmin = QCmin\Delta t$$
$$Cmin\ occurs\ in\ stage\ 1{:}\ 9.95 * 10^{-7} ug/cm^3$$

$$200\ ug = Q\ (7.42 * 10^{-7})(2 * 24 * 60)$$

$$Q = \frac{200\ ug}{\left(7.42 * \frac{10^{-7} ug}{cm^3}\right) * 2880\ minutes} = 93590 \frac{cm^3}{min} = 1560 \frac{cm^3}{s} = .0936 \frac{m^3}{min} = 93.6\ l/mi$$

In order to calculate width, velocity, and pressure drop, we first have to assume length. The following equations were used to calculate these values:

$$Stk50 = .59$$
$$d50\sqrt{Cc} = \left[\frac{9 * \eta * W^2 * L(Stk50)}{\rho pQ}\right]^{\frac{1}{2}}$$
$$d50\sqrt{Cc} = d50 + .078$$

$$Pressure\ drop = .5 * \rho * U^2$$

Given, this information, each stage was designed as shown:

**Stage 1: 5-10 um**

$$Use\ cutpoint\ Dp = 5\ um$$
$$Cc = 1 + 1.7 * Kn/dp$$

$$Cc = 1 + 1.7 * (2 * 0.066)/5) = 1.045$$
$$d50\sqrt{Cc} = \left[\frac{9 * \eta * W^2 * L(Stk50)}{\rho pQ}\right]^{\frac{1}{2}}$$
$$d_{50} = d50\sqrt{Cc} - .078$$
$$d_{50} + .078 = \left[\frac{9 * \eta * W^2 * L(Stk50)}{\rho pQ}\right]^{\frac{1}{2}}$$
$$Assume\ L = 25\ cm$$

$$(5 + .078) * 10^{-4} = \left[\frac{9 * 1.8 * 10^{-4} * W^2 * 25 * 0.59}{1 * 1560}\right]^{1/2}$$
$$W = .13\ cm$$
$$U = \frac{Qmax}{W * L}$$
$$U = \frac{1560\,\frac{cm^3}{s}}{25\ cm * .13\ cm} = 480\ cm^s$$

$$Pressure\ drop = .5 * \rho * U^2 = .5 * 1.2 * 10^{-3}(480^2) = 138.24\,\frac{dyn}{cm^2}$$

**Stage 2: 2.5-5 um**

$$Use\ cutpoint\ Dp = 2.5\ um$$
$$Cc = 1 + 1.7 * Kn/dp$$
$$Cc = 1 + 1.7 * (2 * 0.066)/2.5) = 1.08976$$
$$d_{50} + .078 = \left[\frac{9 * \eta * W^2 * L(Stk50)}{\rho pQ}\right]^{\frac{1}{2}}$$
$$Assume\ L = 15\ cm$$

$$(2.5 + .078) * 10^{-4} = \left[\frac{9 * 1.8 * 10^{-4} * W^2 * 15 * 0.59}{1 * 1560}\right]^{1/2}$$
$$W = .085\ cm$$
$$U = \frac{Qmax}{W * L}$$
$$U = \frac{1560\,\frac{cm^3}{s}}{15\ cm * .085\ cm} = 1223.5\ cm^s$$

$$Pressure\ drop = .5 * \rho * U^2 = .5 * 1.2 * 10^{-3}(1223.5^2) = 898.21\,\frac{dyn}{cm^2}$$

**Stage 3: 1-2.5 um**

$$Use\ cutpoint\ Dp = 1\ um$$

$$Cc = 1 + 1.7 * Kn/dp$$
$$Cc = 1 + 1.7 * (2 * 0.066)/1) = 1.22$$
$$Assume\ L = 10\ cm$$

$$(1 + .078) * 10^{-4} = \left[\frac{9 * 1.8 * 10^{-4} * W^2 * 10 * 0.59}{1 * 1560}\right]^{1/2}$$
$$W = .04\ cm$$
$$U = \frac{Qmax}{W * L}$$
$$U = \frac{1560\,\frac{cm^3}{s}}{10cm * .04\ cm} = 3900\ cm^s$$

$$Pressure\ drop = .5 * \rho * U^2 = .5 * 1.2 * 10^{-3}(3900^2) = 9126\,\frac{dyn}{cm^2}$$

**Stage 4: .5-1 um**

$$Use\ cutpoint\ Dp = .5\ um$$
$$Cc = 1 + 1.7 * Kn/dp$$
$$Cc = 1 + 1.7 * (2 * 0.066)/.5) = 1.45$$
$$d_{50} + .078 = \left[\frac{9 * \eta * W^2 * L(Stk50)}{\rho pQ}\right]^{\frac{1}{2}}$$
$$Assume\ L = 10\ cm$$

$$(.5 + .078) * 10^{-4} = \left[\frac{9 * 1.8 * 10^{-4} * W^2 * 10 * 0.59}{1 * 1560}\right]^{1/2}$$
$$W = .023\ cm$$
$$U = \frac{Qmax}{W * L}$$
$$U = \frac{1560\,\frac{cm^3}{s}}{10\ cm * .023\ cm} = 6782.6\ cm^s$$

$$Pressure\ drop = .5 * \rho * U^2 = .5 * 1.2 * 10^{-3}(6782.6^2) = 27{,}602\,\frac{dyn}{cm^2}$$

**Stage 5: .2-.5**

$$Use\ cutpoint\ Dp = .2\ um$$
$$Cc = 1 + 1.7 * Kn/dp$$
$$Cc = 1 + 1.7 * (2 * 0.066)/.2) = 2.122$$
$$d_{50} + .078 = \left[\frac{9 * \eta * W^2 * L(Stk50)}{\rho pQ}\right]^{\frac{1}{2}}$$
$$Assume\ L = 15\ cm$$

$$(.2 + .078) * 10^{-4} = \left[\frac{9 * 1.8 * 10^{-4} * W^2 * 15 * 0.59}{1 * 1560}\right]^{1/2}$$

$$W = .01\ cm$$

$$U = \frac{Qmax}{W * L}$$

$$U = \frac{1560 \frac{cm^3}{s}}{15\ cm * .01m} = 10{,}400\ cm^s$$

$$Pressure\ drop = .5 * \rho * U^2 = .5 * 1.2 * 10^{-3}(10400^2) = 64{,}896 \frac{dyn}{cm^2}$$

**Stage 6: <.2 um**

$$Everything\ left\ in\ the\ flow$$

In order to verify that this system functions in terms of pressure drop, we must use the figures provided for the selected pump.

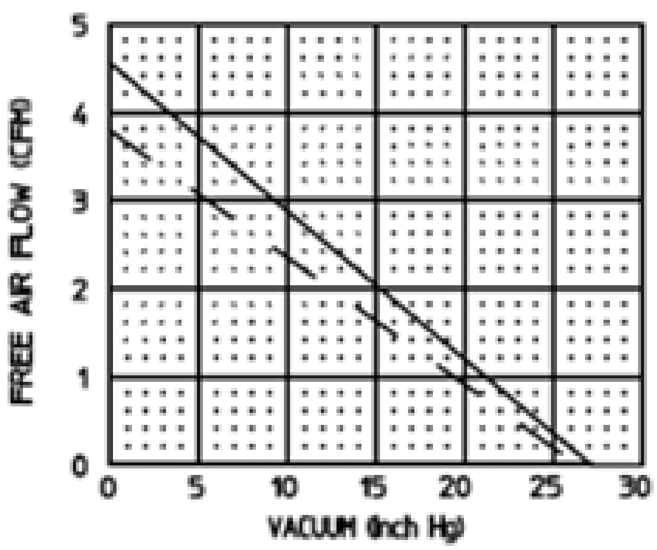


Figure B.1. Pressure chart for the selected pump

Given our flow rate of 3.31 CFM, we can see the maximum pressure is about 6 inches of mercury. Given that we operate the pump at around 85% of the maximum pressure, we can operate at 5.1 inches of mercury. Summing the values for pressure drop at each stage and adding the 10 inches of water drop from the filter results in .122 bar, or about 3.6 inches of mercury. Therefore, the design is feasible with all design parameters shown in the table below.

| Stage | Length (cm) | Width (cm) | U (cm/s) | P (dyn/cm^2) |
|---|---|---|---|---|
| 1 (5-10 um) | 25 | .13 | 480 | 138.20 |
| 2 (2.5-5 um) | 15 | .083 | 1,224 | 898.21 |
| 3 (1-2.5 um) | 10 | .04 | 3,100 | 9,126 |

| | | | | |
|---|---|---|---|---|
| 4 (0.5-1 um) | 10 | .023 | 6,783 | 27,602 |
| 5 (0.2-0.5 um) | 15 | 0.01 | 10,400 | 64,896 |
| 6 (<2) | Remaining flow | Remaining flow | Remaining Flow | Remaining Flow |

Table B.2. Cascade impactor design parameters for each stage.

## *Part C: Respiratory System (Sining Niu)*

*Introduction:*

Human respiratory system is divided into three different regions: head region (HA), tracheobronchial region (TB) and alveolar region (AL). Particles are deposited in respiratory system by interception, impaction and diffusion.

*Calculations and results:*

Respiratory deposition fraction calculations:

Head Region:

$$DF_{HA} = IF\left(\frac{1}{1 + exp(6.84 + 1.183 ln d_p)} + \frac{1}{1 + exp(0.924 - 1.885 ln d_p)}\right)$$

$$IF = 1 - 0.5\left(1 - \frac{1}{1 + 0.00076 {d_p}^{2.8}}\right)$$

Tracheobronchial Region:

$$DF_{HA} = \left(\frac{0.00352}{d_p}\right)[exp(-0.234(ln d_p + 3.40)^2) + 63.9 exp(-0.819(ln d_p - 1.61)^2)]$$

Alveolar Region:

$$DF_{AL} = \left(\frac{0.0155}{d_p}\right)[exp(-0.416(ln d_p + 2.84)^2) + 19.411 exp(-0.482(ln d_p - 1.362)^2)]$$

Mass based deposition:

$$mass\ based\ deposition = DF \times resp.\ rate \times t \times mass\ conc.$$

Below in Table C.1, the final results for deposition fraction and mass-based deposition are shown.

| **Dp range (µm)** | **DF_HA** | **DF_TB** | **DF_AL** | **HA (µg)** | **TB (µg)** | **AL (µg)** | **Total (µg)** |
|---|---|---|---|---|---|---|---|
| <0.2 | 0.021 | 0.027 | 0.142 | 2.10 | 2.63 | 14.09 | 18.82 |
| 0.2 – 0.5 | 0.056 | 0.005 | 0.064 | 16.93 | 1.43 | 19.38 | 37.74 |
| 0.5 – 1 | 0.189 | 0.016 | 0.109 | 26.44 | 2.27 | 15.31 | 44.02 |
| 1 – 2.5 | 0.532 | 0.052 | 0.126 | 12.95 | 1.27 | 3.07 | 17.29 |
| 2.5 – 5 | 0.815 | 0.056 | 0.080 | 19.58 | 1.35 | 1.92 | 22.85 |
| 5 – 10 | 0.863 | 0.026 | 0.033 | 16.33 | 0.50 | 0.62 | 17.45 |

Table C.1. Results for deposition fraction and mass-based deposition.

From the results above, we can see that larger particles are more likely to deposited in head region by impaction. Since the air flow speed is relatively high there. While for smaller and ultrafine particles, they can reach the tracheobronchial and alveolar region due to diffusion, since the air flow is calmer in lower lung. This coronavirus could adhere to small particles and then easily penetrate into our respiratory system by diffusion.

Recalculated with RH = 90%, salt mass fraction = 25% & 75%

First, need to recalculate the mass concentration for each stage with the new diameter (Dp, retrieved from part E) and origin particle number concentration (Ni):

$$Mass\ Conc.\ = Ni \times \frac{\pi}{6} \times {d_p}^3 \times \rho_p$$

Then, recalculate deposition fraction and mass-based deposition with the same method and results are shown below:

| **Respiratory Deposition RH = 90%, Salt = 25%** | | | | | | | | |
|---|---|---|---|---|---|---|---|---|
| Midpoint Dp (µm) | Mass conc. (µg/m$^3$) | DF_HA | DF_TB | DF_AL | HA (µg) | TB (µg) | AL (µg) | Total (µg) |
| 0.100 | 8.52 | 0.021 | 0.026 | 0.141 | 3.61 | 4.50 | 24.09 | 32.20 |
| 0.352 | 26.18 | 0.056 | 0.005 | 0.064 | 29.36 | 2.47 | 33.47 | 65.30 |
| 0.753 | 10.52 | 0.190 | 0.016 | 0.110 | 40.04 | 3.44 | 23.09 | 66.57 |
| 1.758 | 2.26 | 0.534 | 0.052 | 0.126 | 24.10 | 2.36 | 5.68 | 32.14 |
| 3.766 | 0.97 | 0.816 | 0.056 | 0.080 | 15.91 | 1.09 | 1.56 | 18.56 |
| 7.532 | 0.92 | 0.863 | 0.026 | 0.032 | 15.86 | 0.48 | 0.60 | 16.94 |

Table C.2. Results for deposition fraction and mass-based deposition with RH = 90% and salt mass fraction = 25%.

| **Respiratory Deposition RH = 90%, Salt = 75%** | | | | | | | | |
|---|---|---|---|---|---|---|---|---|
| Midpoint Dp (µm) | Mass conc. (µg/m$^3$) | DF_HA | DF_TB | DF_AL | HA (µg) | TB (µg) | AL (µg) | Total (µg) |
| 0.145 | 8.52 | 0.021 | 0.015 | 0.087 | 10.59 | 7.53 | 44.52 | 62.64 |
| 0.507 | 26.18 | 0.102 | 0.007 | 0.084 | 159.76 | 11.46 | 131.96 | 303.18 |
| 1.086 | 10.52 | 0.318 | 0.031 | 0.126 | 200.66 | 19.48 | 79.74 | 299.88 |
| 2.535 | 2.26 | 0.693 | 0.061 | 0.109 | 93.77 | 8.23 | 14.68 | 116.68 |
| 5.432 | 0.97 | 0.870 | 0.041 | 0.053 | 50.87 | 2.41 | 3.07 | 56.35 |
| 10.864 | 0.92 | 0.789 | 0.013 | 0.017 | 43.53 | 0.70 | 0.92 | 45.15 |

Table C.3. Results for deposition fraction and mass-based deposition with RH = 90% and salt mass fraction = 75%.

Similar conclusion can be obtained that larger particle are more likely to deposit in head region. Besides, as particle size increases, from mass-based perspective, much more particle mass would deposit in our lung.

## *Part D: Optical Properties (Marco Kleimans)*

*Introduction:*

Driven by the scattering and the absorption of light, optical properties of particles are in charge of many atmospheric phenomena, such as rainbow and smog formation, and visibility degradation, among others. The latter is the focus of this part.

*Calculations and results:*

In order to calculate visibility, we need to know the **extinction coefficient (Qe)**, which is a coefficient attributed to the attenuation of light due to the combined effects of **absorption** and **scattering (σe).** Since absorption is ignored, we thus have:

$$Q_e = \sigma_e$$

We will use as an example on how the calculations were performed with the unaffected particles midpoint of the first stage (0 – 200 nm)[1]. This value corresponds to a median diameter of 100 nm. All the remaining values will be obtained following this method and the results will be reported in tables/graphs below:

First, we need to find the *size parameter* (α):

$$\alpha = \frac{\pi * d}{\lambda} \quad \text{(where } \lambda \text{ is the mid value of visible light, or 550 nm)}$$

So,

$$\alpha = \frac{\pi * 100}{550} = \mathbf{0.571}$$

Then, we compute *Qe* (the *extinction coefficient*) fhrom the provided website in the description of the project:

Qe (from website): **0.025**[2]

It is important to note that for particles where dp > 4000 nm, the Qe value converges to **2** because of the extinction efficiency paradox.

Next, we calculate the scattering coefficient (σe):

$$\sigma_e = \sum_i \frac{\pi N_i d_i^2 (Q_e)_i}{4}$$

So,

$$\sigma_e = \frac{(16364\,\frac{particles}{cm^3})\left(\frac{100\ cm}{1\ m}\right)^3 (100\ nm)^2 \left(\frac{1\ m}{10^9 nm}\right)^2 (0.025)}{4}$$

$$\sigma_e = \mathbf{3.18 \text{ x } 10^6 m^{-1}}$$

The final step is to determine *visibility* (Lv):

[1] Results for unaffected particles are not reported because they are irrelevant in the analysis. However, the data is available in the attached Excel file (i.e. Excel Part_D_Group_D)

[2] Calculations obtained from http://irina.eas.gatech.edu/Lab_Source/sphere5235.aspx

$$L_v = \frac{-\ln(0.02)}{\sigma_e} = \frac{3.91}{\sigma_e}$$

So,

$$L_v = \frac{3.91}{3.18 \text{ x } 10^6 m^{-1}(\frac{1000m}{1km})}$$

$$L_v = \mathbf{1228.083419\ km}$$

Finally, we calculate overall visibility. For this part, the σe values for each individual midpoint value for each cut-off range have been summed up using the sum function in excel (i.e =sum($\sigma_{0-200}$: $\sigma_{5000-10000}$)) and then the summed value was evaluate using the formula in step 4. For instance:

| **Midpoint (dp [=] nm)** | **Scattering coefficient (σ [=] m^-1)** | **Visibility (Lv [=] km)** |
|---|---|---|
| 100 | 3.18E-06 | 1228.083419 |
| 350 | 2.03E-04 | 19.2996188 |
| 750 | 9.32E-05 | 41.96975745 |
| 1750 | 6.19E-06 | 631.8590341 |
| 3750 | 9.41E-07 | 4152.972698 |
| 7500 | 4.42E-07 | 8854.483129 |
| | Summed σ | 3.07E-04 |
| | Overall Visibility | 12.75643426 |

Table D.1. Summed values for the scattering of light and summation across scattering coefficient column to obtain overall visibility (unaffected particles).

These are the results obtain:

| | **Optical Properties - Salt 25%** | | | | | | |
|---|---|---|---|---|---|---|---|
| | Stage (dp [=] nm) | Midpoint (dp [=] nm) | Ni (particles/cm^3) | α | QE | Scattering coefficient (σ [=] m^-1) | Visibility (Lv [=] km) |
| RH 95% | 0 - 200 | 128.837 | 16364.15385 | 0.736 | 0.068 | 1.44E-05 | 270.68 |
| | 200 - 500 | 450.931 | 1172.06938 | 2.576 | 2.729 | 5.11E-04 | 7.66 |
| | 500 - 1000 | 966.281 | 48.47386 | 5.519 | 3.155 | 1.12E-04 | 34.86 |
| | 1000-2500 | 2254.655 | 8.92E-01 | 12.879 | 2.179 | 7.76E-06 | 504.05 |
| | 2500 - 5000 | 4831.404 | 3.91E-02 | 27.597 | 2.000 | 1.43E-06 | 2726.41 |
| | 5000 - 10000 | 9662.809 | 5.00E-03 | 55.194 | 2.000 | 7.33E-07 | 5334.32 |
| RH 90% | 0 - 200 | 100.4319169 | 16364.15385 | 0.574 | 0.025 | 3.28E-06 | 1192.34 |
| | 200 - 500 | 351.5117093 | 1172.06938 | 2.008 | 1.813 | 2.06E-04 | 18.96 |
| | 500 - 1000 | 753.2393771 | 48.47386 | 4.302 | 4.360 | 9.42E-05 | 41.52 |
| | 1000-2500 | 1757.558547 | 8.92E-01 | 10.039 | 2.840 | 6.14E-06 | 636.48 |
| | 2500 - 5000 | 3766.196886 | 3.91E-02 | 21.512 | 2.133 | 9.29E-07 | 4206.76 |
| | 5000 - 10000 | 7532.393771 | 5.00E-03 | 43.025 | 2.000 | 4.45E-07 | 8778.49 |
| RH 80% | 0 - 200 | 100 | 16364.15385 | 0.571 | 0.025 | 3.18E-06 | 1228.08 |
| | 200 - 500 | 268.254 | 1172.06938 | 1.532 | 0.801 | 5.31E-05 | 73.70 |
| | 500 - 1000 | 574.829 | 48.47386 | 3.283 | 3.644 | 4.58E-05 | 85.30 |
| | 1000-2500 | 1341.268 | 8.92E-01 | 7.661 | 1.796 | 2.26E-06 | 1728.28 |
| | 2500 - 5000 | 2874.146 | 3.91E-02 | 16.417 | 2.499 | 6.34E-07 | 6165.36 |
| | 5000 - 10000 | 5748.292 | 5.00E-03 | 32.834 | 2.000 | 2.59E-07 | 15073.29 |

Table D.2.a. Results for all the parameters for Salt 25%.

| | Optical Properties - Salt 75% | | | | | | |
|---|---|---|---|---|---|---|---|
| | Stage (dp [=] nm) | Midpoint (dp [=] nm) | Ni (particles/cm^3) | α | QE | Scattering coefficient (σ [=] m^-1) | Visibility (Lv [=] km) |
| RH 95% | 0 - 200 | 185.815755 | 16364.15385 | 1.061 | 0.264 | 1.17E-04 | 33.32050816 |
| | 200 - 500 | 650.3551424 | 1172.06938 | 3.715 | 4.178 | 1.63E-03 | 2.40381461 |
| | 500 - 1000 | 1393.618162 | 48.47386 | 7.960 | 1.691 | 1.25E-04 | 31.27352634 |
| | 1000-2500 | 3251.775712 | 8.92E-01 | 18.574 | 2.366 | 1.75E-05 | 223.218674 |
| | 2500 - 5000 | 6968.090812 | 3.91E-02 | 39.802 | 2.000 | 2.98E-06 | 1310.720599 |
| | 5000 - 10000 | 13936.18162 | 5.00E-03 | 79.603 | 2.000 | 1.52E-06 | 2564.47309 |
| RH 90% | 0 - 200 | 144.8478891 | 16364.15385 | 0.827 | 0.106 | 2.87E-05 | 136.31 |
| | 200 - 500 | 506.9676117 | 1172.06938 | 2.896 | 3.362 | 7.95E-04 | 4.92 |
| | 500 - 1000 | 1086.359168 | 48.47386 | 6.205 | 2.477 | 1.11E-04 | 35.13 |
| | 1000-2500 | 2534.838059 | 8.92E-01 | 14.479 | 2.068 | 9.31E-06 | 420.17 |
| | 2500 - 5000 | 5431.79584 | 3.91E-02 | 31.026 | 2.000 | 1.81E-06 | 2157.00 |
| | 5000 - 10000 | 10863.59168 | 5.00E-03 | 62.053 | 2.000 | 9.26E-07 | 4220.26 |
| RH 80% | 0 - 200 | 110.5396 | 16364.15385 | 0.631 | 0.037 | 5.79E-06 | 675.08 |
| | 200 - 500 | 386.8887 | 1172.06938 | 2.210 | 2.087 | 2.88E-04 | 13.60 |
| | 500 - 1000 | 829.0472 | 48.47386 | 4.736 | 3.861 | 1.01E-04 | 38.70 |
| | 1000-2500 | 1934.4435 | 8.92E-01 | 11.050 | 3.014 | 7.90E-06 | 495.10 |
| | 2500 - 5000 | 4145.236 | 3.91E-02 | 23.678 | 2.000 | 1.06E-06 | 3703.73 |
| | 5000 - 10000 | 8290.4721 | 5.00E-03 | 47.355 | 2.000 | 5.40E-07 | 7246.48 |

Table D.2.b. Results for all the parameters for Salt 75%.

| Overall Visibility | | |
|---|---|---|
| **Relative Humidity** | **Salt 25%** | **Salt 75%** |
| 0.95 | 6.040446481 | 2.067714644 |
| 0.9 | 12.56519675 | 4.127158916 |
| 0.8 | 37.15666169 | 9.682361663 |

Table D.3. Overall visibility of both salt types across the different relative humidity values.

From these data, the following trends can be observed. First and foremost, as it can be appreciated from table D.3, that as relative humidity increases, the visibility decreases, and particles which are 75% salt have a greater impact on overall visibility. This trend is illustrated in the following graph:

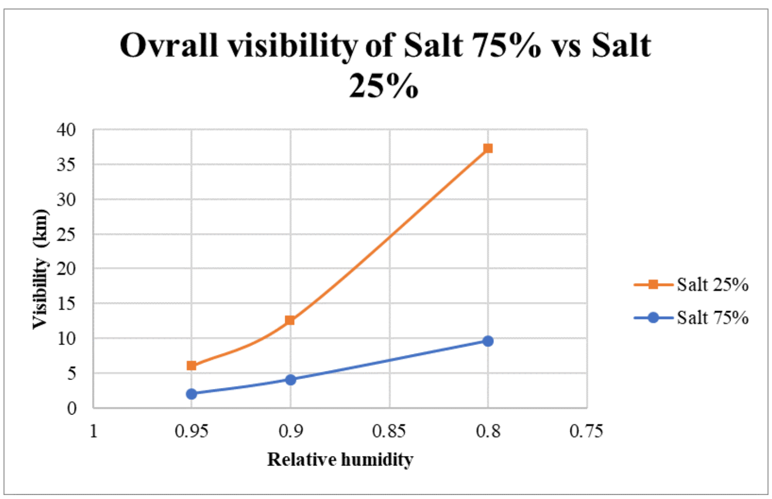


Figure D.1. As it can be seen from this plot, the visibility is affected by both relative humidity and salt percent of each type of particle.

Furthermore, visibility reaches a minimum at the accumulation mode particles. When observing table D.2.a and D.2.b, one can see that the trend is consistent across salt types and humidity conditions. This is because particles of this size do not have effective mechanisms to deposit (i.e. these are to massive for diffusion and too small for gravitational settling) and therefore remain suspended in the air for longer periods of time. This trend can be graphically appreciated below.

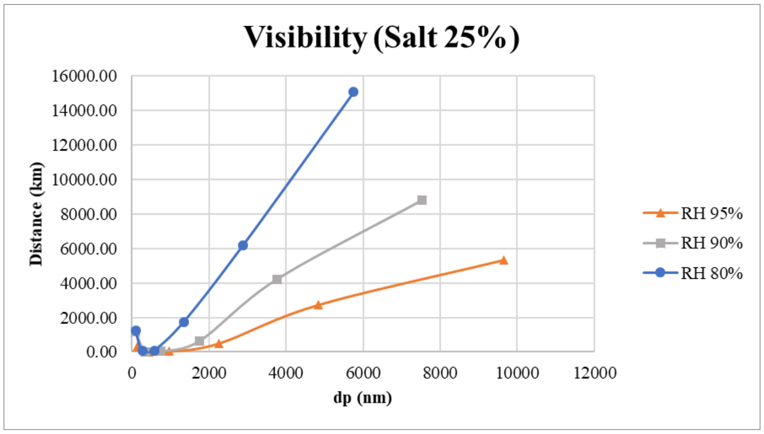


Figure D.2.a. Visibility of salt 25% at the different stages in the different relative humidity conditions.

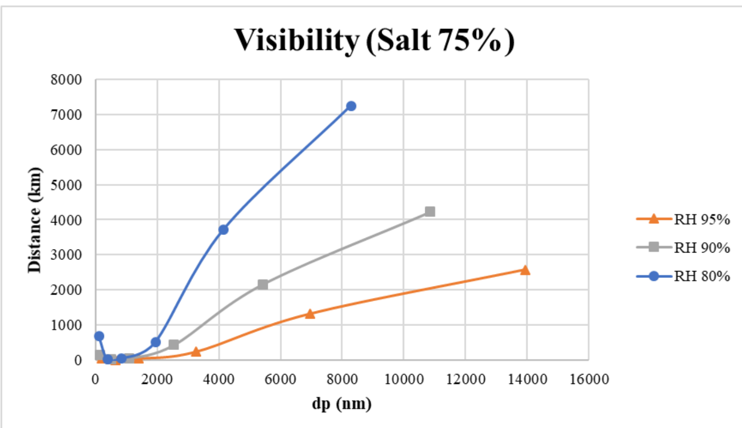


Figure D.2.b. Visibility of salt 75% at the different stages in the different relative humidity conditions.

## *Part E: Condensational growth (Zijiao Zhang)*

*Introduction:*

In this part, we will assume that each size range has hygroscopic components that are 25% and 75% by mass. Then we need to calculate growth in lungs assuming 95% relative humidity in our respiratory tract and redo that for relative humidity equal to 80 and 90%. We also need to calculate surface area and mass or volume concentrations of grown aerosol. For the parts of respiratory deposition, scattering calculations and visibility range calculations, we have calculated the values in the previous parts.

*Calculations and results:*

For the first step, we need to calculate the grown particle diameter. Based on Kohler equation, we can ignore Kelvin effect and just consider the Raoult term. And the equation is posted below.

$$\frac{p}{P_s} = \left(1 + \frac{6im_sM_w}{M_s\rho_\omega \pi {d_{(p,grown)}}^3}\right)^{-1}$$

We already know the number of dissolved ions or i is equal to 2. Molecular weight of water or $M_w$ is equal to 18. Molecular weight of ammonium nitrate or $M_s$ is equal to 80. And the density of water or $\rho_w$ is equal to 1 g/cm$^3$. So we can substitute these given data in different conditions where the salt mass fraction are 25 percent and 75%, and when relative humidity are 95%, 90% and 80%. And then the grown particle diameter or $d_p$ can be calculated.

For example, when the salt percentage is 25% and the relative humidity is 95%, we can get this equation below and calculate grown particle diameter.

$$\frac{p}{Ps} = 95\% = \left(1 + \frac{6im_sM_w}{M_s\rho_w \pi {d_{(p,grown)}}^3}\right)^{-1} = （1 + \frac{6 \times 2 \times 25\% \times 1.72 \times \frac{\pi}{6} {d_p}^3 \times 18}{80 \times 1 \times \pi \times {d_{(p,grown)}}^3}）^{-1}$$

So these are results when the salt mass fraction is 25% as table E.1.(a). shows. We can see the grown particle diameters for different relative humidity.

| $d_p$ (µm) | $m_s$ (g) | $d_{(p,grown)}$, 80% RH (µm) | $d_{(p,grown)}$, 90% RH (µm) | $d_{(p,grown)}$, 95% RH (µm) |
|---|---|---|---|---|
| 0.1 | 1.309E-16 | 0.08 | 0.10 | 0.13 |
| 0.35 | 5.61232E-15 | 0.27 | 0.35 | 0.45 |
| 0.75 | 5.52233E-14 | 0.57 | 0.75 | 0.97 |
| 1.75 | 7.01541E-13 | 1.34 | 1.76 | 2.25 |
| 3.75 | 6.90291E-12 | 2.87 | 3.77 | 4.83 |
| 7.5 | 5.52233E-11 | 5.75 | 7.53 | 9.66 |

Table E.1.(a). Results of grown diameter for salt 25%.

And these are results when the condition is 75% hygroscopic components for different relative humidity as table E.1.(b). shows.

| $d_p$ (μm) | $m_s$ (g) | $d_{(p,grown)}$, 80% RH (μm) | $d_{(p,grown)}$, 90% RH (μm) | $d_{(p,grown)}$, 95% RH (μm) |
|---|---|---|---|---|
| 0.1 | 3.92699E-16 | 0.11 | 0.14 | 0.19 |
| 0.35 | 1.6837E-14 | 0.39 | 0.51 | 0.65 |
| 0.75 | 1.6567E-13 | 0.83 | 1.09 | 1.39 |
| 1.75 | 2.10462E-12 | 1.93 | 2.53 | 3.25 |
| 3.75 | 2.07087E-11 | 4.15 | 5.43 | 6.97 |
| 7.5 | 1.6567E-10 | 8.29 | 10.86 | 13.94 |

Table E.1.(b). Results of grown diameter for salt 75%.

Compare with these two charts, we can conclude that in the same salt percentage, the grown particle diameter also increases with the relative humidity increasing. And in the same relative humidity percentage, with the salt percentage increasing, grown particle diameter is increasing too.

For part of mass or volume concentrations and surface area of grown aerosol calculations, the number concentration of the particles stays the same as part A. We already know the equations of volume concentrations and surface area as follows.

For every particle size:

$$dN = \frac{dN}{dlogd_p} \times (\log D_{p,u} - \log D_{p,l})$$

$$\text{Mass concentration } = dN \times \frac{\pi}{6} \times {d_p}^3 \times \rho_p$$

$$\text{Volume concentration} = \mathrm{dN} \times \frac{\pi}{6} \times \mathrm{d_p}^3$$

$$\text{Surface area} = \pi \times \mathrm{d_p}^2 \times dN$$

Total mass concentration, volume concentration and surface area are given by following equations:

$$\text{Total mass concentration} = \sum Mass\ concentration\ of\ every\ particle\ size$$

$$\text{Total volume concentration} = \sum Volume\ concentration\ of\ every\ particle\ size$$

$$\text{Total surface area} = \sum Surface\ area\ of\ every\ particle\ size$$

So we can get the values for 25% hygroscopic components and for different relative humidity which are 80% and 90% as table E.2.(a). shows.

| | RH = 80% | | | RH = 90% | | |
|---|---|---|---|---|---|---|
| **$d_p$ (µm)** | **$d_{(p,grown)}$ (µm)** | **Volume Concentration ($µm^3/m^3$)** | **Surface Area ($µm^2/m^3$)** | **$d_{(p,grown)}$ (µm)** | **Volume Concentration ($µm^3/m^3$)** | **Surface Area ($µm^2/m^3$)** |
| 0.1 | 0.08 | 3.77E+06 | 2.95E+08 | 0.10 | 8.49E+06 | 5.07E+08 |
| 0.35 | 0.27 | 1.12E+07 | 2.50E+08 | 0.35 | 2.52E+07 | 4.29E+08 |
| 0.75 | 0.57 | 4.18E+06 | 4.36E+07 | 0.75 | 9.40E+06 | 7.49E+07 |
| 1.75 | 1.34 | 6.63E+05 | 2.97E+06 | 1.76 | 1.49E+06 | 5.09E+06 |
| 3.75 | 2.87 | 3.26E+05 | 6.80E+05 | 3.77 | 7.33E+05 | 1.17E+06 |
| 7.5 | 5.75 | 3.50E+05 | 3.65E+05 | 7.53 | 7.88E+05 | 6.27E+05 |

Table E.2.(a). Results for 25% hygroscopic components and for different relative humidity.

And next chart is the results for 75% hygroscopic components and for different relative humidity which are 80% and 90% as table E.2.(b). shows.

| | RH = 80% | | | RH = 90% | | |
|---|---|---|---|---|---|---|
| **$d_p$ (µm)** | **$d_{(p,grown)}$ (µm)** | **Volume Concentration ($µm^3/m^3$)** | **Surface Area ($µm^2/m^3$)** | **$d_{(p,grown)}$ (µm)** | **Volume Concentration ($µm^3/m^3$)** | **Surface Area ($µm^2/m^3$)** |
| 0.1 | 0.08 | 3.77E+06 | 2.95E+08 | 0.10 | 8.49E+06 | 5.07E+08 |
| 0.35 | 0.27 | 1.12E+07 | 2.50E+08 | 0.35 | 2.52E+07 | 4.29E+08 |
| 0.75 | 0.57 | 4.18E+06 | 4.36E+07 | 0.75 | 9.40E+06 | 7.49E+07 |
| 1.75 | 1.34 | 6.63E+05 | 2.97E+06 | 1.76 | 1.49E+06 | 5.09E+06 |
| 3.75 | 2.87 | 3.26E+05 | 6.80E+05 | 3.77 | 7.33E+05 | 1.17E+06 |
| 7.5 | 5.75 | 3.50E+05 | 3.65E+05 | 7.53 | 7.88E+05 | 6.27E+05 |

Table E.2.(b). Results for 75% hygroscopic components and for different relative humidity.

## *Part F: Electrostatic Precipitator (Marco Kleimans)*

*Introduction:*

Electrostatic precipitators take advantage of the electrical properties of aerosols to concentrate particles of desired sizes. The objective of this part is to analyze the parameters for the design of an electrostatic precipitator.

*Calculations and results:*

In order to begin the calculations, the following assumptions were made:

1. Electric field [V/m] = 60,000
2. Dielectric constant (ε) = 5
3. Minimum collection efficiency = 85%
4. Plate Height [m] = 5
5. Plate Width [m] = 6
6. Distance between plates [m] = 0.2
7. Flow rate [m^3/s] = 250
8. Energy cost [$/kWh] = 0.12

These were data given in the problem statement. There are also other fundamental variables that need to be considered. These are the following:

| **Variables** | |
|---|---|
| ***k-constant (ft)*** | 0.6 |
| ***Ion mobility (m^2/V)*** | 1.50E-04 |
| ***Charge on an electron (C)*** | 1.60E-19 |
| ***Mean Thermal Speed of Ions (m/s)*** | 240 |
| ***Proportionality Constant Ke (N*m^2/C^2)*** | 9.00E+09 |
| ***Ni*t (ions/m^3)*** | 1E+13 |
| ***Boltzmann constant (m^2*kg*s^-2*K^-1)*** | 1.38E-23 |
| ***Temperature (K)*** | 293 |
| ***Mean Free Path*** | 0.066 |
| ***Viscosity of air (kg/(m·s))*** | 1.80E-05 |
| ***Surface area total (m)*** | 60 |

Table F.1. Important constants required for calculations.

The following steps were followed for the design of the ESP. First, we computed the power to reach 85% efficiency:

$$E = 1 - \exp\left(-\frac{kPc}{Q}\right) \Rightarrow \mathrm{Pc} = \frac{-Q}{k}\ln(1-E)$$

So,

$$\mathrm{Pc} = -\frac{8827\frac{ft^3}{s}}{0.6}\ln(1-0.85)$$

**Pc= 27910 W**

Then, we determined the potential (dW [V]) and the current (I [A]) in the ESP:

a. dW = $\vec{E} * dx = (60{,}000)(0.2) = \mathbf{12{,}000V}$

b. I = $\frac{Pc}{dW} = \frac{27{,}910}{12{,}000} = \mathbf{2.3A}$

At this point, we will use as an example on how the calculations were performed with the midpoint of the unaffected particle at the first stage (0 – 200 nm)[3], similar to part D. This value corresponds to a median diameter of 100 nm. All of the remaining values will follow this method and the results will be reported in tables/graphs below. The following calculation methods are applicable for all size ranges, across the different types of salt and humidity conditions.

First, to calculate the diffusion and the field charging, we assumed an initial concertation (Nit [#*s*cm$^{-3}$]) of $10^{13}$. Total charging was obtained from the addition of field charging $n_f(t)$ and diffusion charging $n_d(t)$ as follows:

$$n(t) = \frac{d_p kT}{2K_E e^2} \ln\left[1 + \frac{\pi \, K_E d_p \bar{c}_i e^2 N_i t}{2kT}\right]$$

So,

$$n_d(t) = \frac{(100\,nm)(\frac{10^{-9}m}{1\,nm})(1.38x10^{-23})(293K)}{2(9x10^9)(1.6x10^{-19})^2} \ln\left[1 + \frac{\pi\,(9x10^9)(100\,nm)\left(\frac{10^{-9}m}{1\,nm}\right)(240)(1.6x10^{-19})^2(\mathbf{10^{13}})}{2(1.38x10^{-23})(293K)}\right]$$

$n_d(t) = \mathbf{2.73}$

And,

$$n(t) = \left(\frac{3\varepsilon}{\varepsilon + 2}\right)\left(\frac{Ed_p^2}{4K_E e}\right)\left(\frac{\pi K_E e Z_i N_{i\infty} t}{1 + \pi K_E e Z_i N_{i\infty} t}\right)$$

So,

$$n_f(t) = \left(\frac{3*5}{5+2}\right)\left(\frac{(100\,nm)^2\left(\frac{10^{-9}m}{1\,nm}\right)^2(60{,}000)}{4(9x10^9)(1.6x10^{-19})}\right)\left(\frac{\pi\,(9x10^9)(1.6x10^{-19})(1.5x10^{-4})(\mathbf{10^{13}})}{1+\pi\,(9x10^9)(1.6x10^{-19})(1.5x10^{-4})(\mathbf{10^{13}})}\right)$$

$n_f(t) = \mathbf{0.19}$

Thus, the total charge concentration is:

$n(t) = n_d(t) + n_f(t) = 2.73 + 0.19$

$\boldsymbol{n(t) = 2.93}$

[3]Results for unaffected particles are not reported because they are irrelevant in the analysis. However, the data is available in the attached Excel file (i.e. Excel Part_F_Group_D)

Next, we needed to calculate the total area of the plates (Ap) in order to have the targeted collection efficiency of 85%. To do so, we were required to determine the following first:

a. Charge (q):

q = e * n(t) = $(1.6x10^{-19}) * 2.93 = 4.68x10^{-19}C$

b. Slip Correction Factor (Cc):

Cc = $1 + \frac{2.52\lambda}{d} = 1 + \frac{2.52\ (0.066)}{100\ nm\ (\frac{10^{-3}\mu m}{1\ nm})}$

Cc = **2.66**

c. Particle mobility (B)

B = $\frac{C_c}{3\pi\eta d} = \frac{2.66}{3\pi(1.8x10^{-5})(100nm)\left(\frac{10^{-9}m}{1\ nm}\right)}$

**B = $\mathbf{1.57\ x\ 10^{11}\ \frac{N}{m*s}}$**

d. Electric mobility (Z)

Z = qB = $(4.68x10^{-19})(1.57\ x\ 10^{11})$

**Z = $\mathbf{7.35\ x\ 10^{-8}\ \frac{m^2}{V*s}}$**

e. Settling velocity (Vte)

$V_{TE} = ZE = 7.35\ x\ 10^{-8} * 60{,}000$

$\boldsymbol{V_{TE} = 0.0044\frac{m}{s}}$

It is important to note that many of these calculations can be replaced by data in Appendix A.11 from Hinds, but since the diameter sizes are specific, these cannot be located on the table. Therefore, for the sake of consistency, all the values were derived from calculations.

Once settling velocity was obtained, the preferred total plate area was calculated:

$$E = 1 - \exp\left(-\frac{V_{TE}A_c}{Q}\right) \implies A_P = -\frac{Q}{V_{TE}}\ln(1-E)$$

$A_P = -\frac{250}{0.0044}\ln(1 - 0.85)$

$\boldsymbol{A_P = 107527\ m^2}$

After having found the areas for each of the range sizes, the largest value was selected, which corresponded to $\mathbf{126689\ m^2}$ for the 200-500nm stage. This can be observed in the following table.

| Stage (dp [=] nm) | Settling Velocity (V/m) | Ac (m) |
|---|---|---|
| 100 - 200 | 0.0044 | 107527.2242 |
| 200 - 500 | 0.0037 | 126689.0246 |
| 500 - 1000 | 0.0041 | 115767.8007 |
| 1000-2500 | 0.0053 | 88875.79008 |
| 2500 - 5000 | 0.0078 | 60933.65102 |
| 5000 - 10000 | 0.0122 | 38907.75067 |

Table F.2. Different plate areas for each stage given the corresponding settling velocity (unaffected particles). The largest area (200-500 nm) was selected.

Now, we computed the new ion concentration:

$$N_i = \frac{I}{A_p * E * Z_i * e}$$

So,

$$N_i = \frac{2.3}{(126689)(250)*(1.5x10^{-4})*(1.5x10^{-19})}$$

$$\boldsymbol{N_i = 1.27x10^{13}}$$

We also found the number of plates:

$$\text{Np} = \frac{A_p}{2 * Area\ of\ single\ plate} = \frac{126689}{30*2}$$

**Np = 2112**

Then, we evaluated the airflow velocity:

U = Q/(number of plates-1)/(H *Dx)

So,

U = 250/(2112 – 1)/(5*0.2)

**U = 0.118 m/s**

Next, we calculated the residence time:

τ = L/U = 6/0.118

**τ = 50.6 s**

Once we obtained the new particle concentration (Ni) and the residence time (τ), we were able to calculate the new particle concentration Nit:

Nit = Ni*τ = $1.27x10^{13}$ * 50.6

**Nit (new) =** $\boldsymbol{6.5x10^{14}}$

When the new Nit is obtained, the calculations are repeated, from the evaluation of the total charges to the computation of – once again – a second Nit. When calculating the plate area, we updated to the new efficiency (97%) and the most-recently calculated terminal velocity ($V_{te}$), corresponding to the previously calculated plate area. This way we can confirm that our updated efficiency is correct (the Nit from both steps must match):

**Nit (check) = $\mathbf{6.5x10^{14}}$**

At this point, as stated before, we also calculated the updated efficiency:

$$E = 1 - \exp\left(-\frac{V_{TE} A_c}{Q}\right)$$

where $V_{te}$ comes from the latest iteration with the latest Nit value and the plate area ($A_p$) corresponds to the value from the first iteration.

$$\mathrm{E} = 1 - exp\ (-\frac{(0.069)(126689)}{(250)})$$

**E = 97%**

Finally, we estimated the purchasing and cost with the updated particle concentration and plate area:

Purchasing $cost = a * A_p^b$ where a = 96.0 and b = 0.63 and Ap in $ft^2$

So,

Purchasing cost = 96* ( $128598m^2 * 10.7639\,\frac{ft^2}{m^2})^2$

**Purchasing cost = $709,953.61**

Similarly, we can calculated the operational costs:

Operational cost $= Pc\ * \frac{\$}{kWh}\ * hr$

So,

Daily operational cost = $27910\ W\ \left(\frac{1\ kW}{1000\ W}\right)\left(\frac{\$0.12}{1\ kWh}\right)(24hr)$

**Daily operational cost (DOC) = $80.40**

And,

Yearly operational cost = DOC * 365

So,

Yearly operational cost = $80.40 * 365

**Yearly operational cost (YOC) = $29,344.32**

These are the results obtained for every particle type at different relative humidity conditions:

| | | SALT 25% | | | | | | | | | | | |
|---|---|---|---|---|---|---|---|---|---|---|---|---|---|
| | | Stage (dp [=] nm) | Midpoint (dp [=] nm) | Midpoint (dp [=] m) | Diffusion Charging | Field Charging | Total Charges | Charge (C) | Particle Mobility (m/N*s) | Slip Correction | Electric Mobility (m^2/V*s) | Settling Velocity (V/m) | Ac (m) |
| RH - 95% | First iteration | 100 - 200 | 128.837 | 1.29E-07 | 3.80 | 0.32 | 4.12 | 6.58923E-19 | 1.04816E+11 | 2.290933505 | 6.90658E-08 | 0.004143947 | 114451.27 |
| | | 200 - 500 | 450.931 | 4.51E-07 | 18.14 | 3.96 | 22.10 | 3.53584E-18 | 17893610699 | 1.368836917 | 6.32689E-08 | 0.003796134 | 124937.65 |
| | | 500 - 1000 | 966.281 | 9.66E-07 | 45.30 | 18.16 | 63.46 | 1.01538E-17 | 7150335637 | 1.172123844 | 7.26034E-08 | 0.004356204 | 108874.60 |
| | | 1000-2500 | 2254.655 | 2.25E-06 | 122.41 | 98.90 | 221.31 | 3.54089E-17 | 2807284827 | 1.073767383 | 9.94028E-08 | 0.00596417 | 79521.54 |
| | | 2500 - 5000 | 4831.404 | 4.83E-06 | 294.58 | 454.12 | 748.70 | 1.19792E-16 | 1262065593 | 1.034424776 | 1.51185E-07 | 0.009071127 | 52284.57 |
| | | 5000 - 10000 | 9662.809 | 9.66E-06 | 647.93 | 1816.46 | 2464.39 | 3.94303E-16 | 620532614 | 1.017212386 | 2.44678E-07 | 0.014680657 | 32306.46 |
| | | Stage (dp [=] nm) | Midpoint (dp [=] nm) | Midpoint (dp [=] m) | Diffusion Charging | Field Charging | Total Charges | Charge (C) | Particle Mobility (m/N*s) | Slip Correction | Electric Mobility (m^2/V*s) | Settling Velocity (V/m) | Ac (m) |
| | Second iteration | 100 - 200 | 128.837 | 1.29E-07 | 8.47 | 0.37 | 8.84 | 1.41E-18 | 1.05E+11 | 2.290933505 | 1.48E-07 | 0.0089 | 94417.61756 |
| | | 200 - 500 | 450.931 | 4.51E-07 | 34.60 | 4.53 | 39.13 | 6.26E-18 | 1.79E+10 | 1.37 | 1.12E-07 | 0.0067 | 124937.6456 |
| | | 500 - 1000 | 966.281 | 9.66E-07 | 80.61 | 20.79 | 101.41 | 1.62E-17 | 7.15E+09 | 1.17 | 1.16E-07 | 0.0070 | 120647.4815 |
| | | 1000-2500 | 2254.655 | 2.25E-06 | 204.86 | 113.21 | 318.08 | 5.09E-17 | 2.81E+09 | 1.07 | 1.43E-07 | 0.0086 | 97969.3398 |
| | | 2500 - 5000 | 4831.404 | 4.83E-06 | 471.32 | 519.85 | 991.17 | 1.59E-16 | 1.26E+09 | 1.03 | 2.00E-07 | 0.0120 | 69932.23786 |
| | | 5000 - 10000 | 9662.809 | 9.66E-06 | 1001.44 | 2079.40 | 3080.84 | 4.93E-16 | 6.21E+08 | 1.02 | 3.06E-07 | 0.0184 | 45758.70761 |
| | | Stage (dp [=] nm) | Midpoint (dp [=] nm) | Midpoint (dp [=] m) | Diffusion Charging | Field Charging | Total Charges | Charge (C) | Particle Mobility (m/N*s) | Slip Correction | Electric Mobility (m^2/V*s) | Settling Velocity (V/m) | Ac (m) |
| RH - 90% | First iteration | 100 - 200 | 100.4319169 | 1.00E-07 | 2.75 | 0.20 | 2.94 | 4.71018E-19 | 1.55891E+11 | 2.656047252 | 7.34273E-08 | 0.004405641 | 107652.90 |
| | | 200 - 500 | 351.5117093 | 3.52E-07 | 13.38 | 2.40 | 15.79 | 2.52594E-18 | 24703894008 | 1.473156358 | 6.24006E-08 | 0.003744033 | 126676.22 |
| | | 500 - 1000 | 753.2393771 | 7.53E-07 | 33.67 | 11.04 | 44.71 | 7.15358E-18 | 9553667313 | 1.2208063 | 6.83429E-08 | 0.004100575 | 115661.83 |
| | | 1000-2500 | 1757.558547 | 1.76E-06 | 91.59 | 60.10 | 151.68 | 2.42691E-17 | 3671253871 | 1.094631271 | 8.90982E-08 | 0.005345891 | 88718.61 |
| | | 2500 - 5000 | 3766.196886 | 3.77E-06 | 221.41 | 275.95 | 497.36 | 7.95771E-17 | 1634259144 | 1.04416126 | 1.3005E-07 | 0.007802978 | 60781.92 |
| | | 5000 - 10000 | 7532.393771 | 7.53E-06 | 488.61 | 1103.79 | 1592.40 | 2.54784E-16 | 799849927.5 | 1.02208063 | 2.03789E-07 | 0.012227358 | 38788.43 |
| | | Stage (dp [=] nm) | Midpoint (dp [=] nm) | Midpoint (dp [=] m) | Diffusion Charging | Field Charging | Total Charges | Charge (C) | Particle Mobility (m/N*s) | Slip Correction | Electric Mobility (m^2/V*s) | Settling Velocity (V/m) | Ac (m) |
| | Second iteration | 100 - 200 | 100.4319169 | 1.00E-07 | 6.38 | 0.22 | 6.61 | 1.06E-18 | 1.56E+11 | 2.656047252 | 1.65E-07 | 0.0099 | 87971.33066 |
| | | 200 - 500 | 351.5117093 | 3.52E-07 | 26.20 | 2.75 | 28.96 | 4.63E-18 | 2.47E+10 | 1.47 | 1.14E-07 | 0.0069 | 126676.2248 |
| | | 500 - 1000 | 753.2393771 | 7.53E-07 | 61.19 | 12.64 | 73.83 | 1.18E-17 | 9.55E+09 | 1.22 | 1.13E-07 | 0.0068 | 128474.6413 |
| | | 1000-2500 | 1757.558547 | 1.76E-06 | 155.85 | 68.79 | 224.65 | 3.59E-17 | 3.67E+09 | 1.09 | 1.32E-07 | 0.0079 | 109872.7077 |
| | | 2500 - 5000 | 3766.196886 | 3.77E-06 | 359.17 | 315.89 | 675.06 | 1.08E-16 | 1.63E+09 | 1.04 | 1.77E-07 | 0.0106 | 82137.63957 |
| | | 5000 - 10000 | 7532.393771 | 7.53E-06 | 764.17 | 1263.57 | 2027.74 | 3.24E-16 | 8.00E+08 | 1.02 | 2.60E-07 | 0.0156 | 55870.89967 |
| | | Stage (dp [=] nm) | Midpoint (dp [=] nm) | Midpoint (dp [=] m) | Diffusion Charging | Field Charging | Total Charges | Charge (C) | Particle Mobility (m/N*s) | Slip Correction | Electric Mobility (m^2/V*s) | Settling Velocity (V/m) | Ac (m) |
| RH - 80% | First iteration | 100 - 200 | 100 | 1.00E-07 | 2.73 | 0.19 | 2.93 | 4.68279E-19 | 1.56986E+11 | 2.6632 | 7.35132E-08 | 0.00441079 | 107527.22 |
| | | 200 - 500 | 268.254 | 2.68E-07 | 9.59 | 1.40 | 10.99 | 1.75781E-18 | 35598171733 | 1.620009394 | 6.25748E-08 | 0.003754491 | 126323.39 |
| | | 500 - 1000 | 574.829 | 5.75E-07 | 24.34 | 6.43 | 30.77 | 4.92326E-18 | 13221616446 | 1.289338221 | 6.50934E-08 | 0.003905607 | 121435.67 |
| | | 1000-2500 | 1341.268 | 1.34E-06 | 66.72 | 35.00 | 101.72 | 1.62751E-17 | 4939783473 | 1.124002064 | 8.03955E-08 | 0.004823727 | 98322.31 |
| | | 2500 - 5000 | 2874.146 | 2.87E-06 | 162.16 | 160.71 | 322.86 | 5.16583E-17 | 2169595981 | 1.057867624 | 1.12078E-07 | 0.006724663 | 70528.45 |
| | | 5000 - 10000 | 5748.292 | 5.75E-06 | 359.25 | 642.83 | 1002.08 | 1.60333E-16 | 1055127604 | 1.028933812 | 1.69172E-07 | 0.010150325 | 46725.59 |
| | | Stage (dp [=] nm) | Midpoint (dp [=] nm) | Midpoint (dp [=] m) | Diffusion Charging | Field Charging | Total Charges | Charge (C) | Particle Mobility (m/N*s) | Slip Correction | Electric Mobility (m^2/V*s) | Settling Velocity (V/m) | Ac (m) |
| | Second iteration | 100 - 200 | 100 | 1.00E-07 | 6.35 | 0.22 | 6.57 | 1.05E-18 | 1.57E+11 | 2.6632 | 1.65E-07 | 0.0099 | 91341.62161 |
| | | 200 - 500 | 268.254 | 2.68E-07 | 19.36 | 1.60 | 20.96 | 3.35E-18 | 3.56E+10 | 1.62 | 1.19E-07 | 0.0072 | 126323.3866 |
| | | 500 - 1000 | 574.829 | 5.75E-07 | 45.33 | 7.36 | 52.69 | 8.43E-18 | 1.32E+10 | 1.29 | 1.11E-07 | 0.0067 | 135316.4068 |
| | | 1000-2500 | 1341.268 | 1.34E-06 | 115.76 | 40.06 | 155.82 | 2.49E-17 | 4.94E+09 | 1.12 | 1.23E-07 | 0.0074 | 122477.33 |
| | | 2500 - 5000 | 2874.146 | 2.87E-06 | 267.28 | 183.97 | 451.25 | 7.22E-17 | 2.17E+09 | 1.06 | 1.57E-07 | 0.0094 | 96292.80256 |
| | | 5000 - 10000 | 5748.292 | 5.75E-06 | 569.53 | 735.88 | 1305.42 | 2.09E-16 | 1.06E+09 | 1.03 | 2.20E-07 | 0.0132 | 68443.82808 |

Table F.3.a.1. Salt 25% calculation results for the different relative humidity conditions.

| | Salt 25% | | | | | |
|---|---|---|---|---|---|---|
| | RH 95% | | RH 90% | | RH 90% | |
| | First iteration | Second iteration | First iteration | Second iteration | First iteration | Second iteration |
| **Concentration (Ni)** | 1.29E+13 | 1.29E+13 | 1.28E+13 | 1.26E+13 | 1.28E+13 | 1.19E+13 |
| **Number of plates** | 2082.294093 | 2082.294093 | 2111.270414 | 2141.244022 | 2105.389776 | 2255.273446 |
| **Velocity (m/s)** | 0.120117575 | 0.120117575 | 0.11846823 | 0.11680911 | 0.118799285 | 0.110900477 |
| **t (s)** | 49.95105823 | 49.95105823 | 50.64648994 | 51.36585654 | 50.50535464 | 54.10256271 |
| **NiT New** | 6.5E+14 | 6.5E+14 | 6.5E+14 | 6.5E+14 | 6.5E+14 | 6.5E+14 |

Table F.3.a.2. Salt 25% updated Nit and Nit check calculations.

| | | SALT 75% | | | | | | | | | | | |
|---|---|---|---|---|---|---|---|---|---|---|---|---|---|
| | | Stage (dp [=] nm) | Midpoint (dp [=] nm) | Midpoint (dp [=] m) | Diffusion Charging | Field Charging | Total Charges | Charge (C) | Particle Mobility (m/N*s) | Slip Correction | Electric Mobility (m^2/V*s) | Settling Velocity (V/m) | Ac (m) |
| RH - 95% | First iteration | 100 - 200 | 128.837 | 1.29E-07 | 3.80 | 0.32 | 4.12 | 6.58923E-19 | 60117570792 | 1.895080183 | 3.96129E-08 | 0.002376771 | 199548.02 |
| | | 200 - 500 | 450.931 | 4.51E-07 | 18.14 | 3.96 | 22.10 | 3.53584E-18 | 11381632201 | 1.255737195 | 4.02436E-08 | 0.002414616 | 196420.47 |
| | | 500 - 1000 | 966.281 | 9.66E-07 | 45.30 | 18.16 | 63.46 | 1.01538E-17 | 4734522175 | 1.119344024 | 4.80736E-08 | 0.002884417 | 164428.40 |
| | | 1000-2500 | 2254.655 | 2.25E-06 | 122.41 | 98.90 | 221.31 | 3.54089E-17 | 1905458178 | 1.051147439 | 6.74702E-08 | 0.00404821 | 117157.97 |
| | | 2500 - 5000 | 4831.404 | 4.83E-06 | 294.58 | 454.12 | 748.70 | 1.19792E-16 | 866137569 | 1.023868805 | 1.03756E-07 | 0.006225385 | 76184.85 |
| | | 5000 - 10000 | 9662.809 | 9.66E-06 | 647.93 | 1816.46 | 2464.39 | 3.94303E-16 | 428020855.4 | 1.011934402 | 1.6877E-07 | 0.010126184 | 46836.99 |
| | | Stage (dp [=] nm) | Midpoint (dp [=] nm) | Midpoint (dp [=] m) | Diffusion Charging | Field Charging | Total Charges | Charge (C) | Particle Mobility (m/N*s) | Slip Correction | Electric Mobility (m^2/V*s) | Settling Velocity (V/m) | Ac (m) |
| | Second iteration | 100 - 200 | 128.837 | 1.29E-07 | 8.47 | 0.37 | 8.84 | 1.41E-18 | 6.01E+10 | 1.895080183 | 8.50E-08 | 0.0051 | 164618.1986 |
| | | 200 - 500 | 450.931 | 4.51E-07 | 34.60 | 4.53 | 39.13 | 6.26E-18 | 1.14E+10 | 1.26 | 7.13E-08 | 0.0043 | 196420.474 |
| | | 500 - 1000 | 966.281 | 9.66E-07 | 80.61 | 20.79 | 101.41 | 1.62E-17 | 4.73E+09 | 1.12 | 7.68E-08 | 0.0046 | 182209.0094 |
| | | 1000-2500 | 2254.655 | 2.25E-06 | 204.87 | 113.21 | 318.08 | 5.09E-17 | 1.91E+09 | 1.05 | 9.70E-08 | 0.0058 | 144337.8236 |
| | | 2500 - 5000 | 4831.404 | 4.83E-06 | 471.33 | 519.85 | 991.18 | 1.59E-16 | 8.66E+08 | 1.02 | 1.37E-07 | 0.0082 | 101900.6224 |
| | | 5000 - 10000 | 9662.809 | 9.66E-06 | 1001.45 | 2079.40 | 3080.86 | 4.93E-16 | 4.28E+08 | 1.01 | 2.11E-07 | 0.0127 | 66340.52811 |
| | | Stage (dp [=] nm) | Midpoint (dp [=] nm) | Midpoint (dp [=] m) | Diffusion Charging | Field Charging | Total Charges | Charge (C) | Particle Mobility (m/N*s) | Slip Correction | Electric Mobility (m^2/V*s) | Settling Velocity (V/m) | Ac (m) |
| RH - 90% | First iteration | 100 - 200 | 144.8478891 | 1.45E-07 | 4.41 | 0.41 | 4.82 | 7.71074E-19 | 87423220329 | 2.148239032 | 6.74098E-08 | 0.004044585 | 117262.95 |
| | | 200 - 500 | 506.9676117 | 5.07E-07 | 20.91 | 5.00 | 25.91 | 4.14626E-18 | 15441751588 | 1.328068295 | 6.40256E-08 | 0.003841535 | 123461.07 |
| | | 500 - 1000 | 1086.359168 | 1.09E-06 | 52.04 | 22.96 | 75.00 | 1.19996E-17 | 6256757964 | 1.153098538 | 7.50787E-08 | 0.004504724 | 105285.04 |
| | | 1000-2500 | 2534.838059 | 2.53E-06 | 140.22 | 125.00 | 265.23 | 4.24361E-17 | 2478026389 | 1.065613659 | 1.05158E-07 | 0.00630946 | 75169.66 |
| | | 2500 - 5000 | 5431.79584 | 5.43E-06 | 336.77 | 573.99 | 910.77 | 1.45723E-16 | 1118436604 | 1.030619708 | 1.62981E-07 | 0.009778886 | 48500.41 |
| | | 5000 - 10000 | 10863.59168 | 1.09E-05 | 739.61 | 2295.97 | 3035.58 | 4.85693E-16 | 550911115.2 | 1.015309854 | 2.67574E-07 | 0.016054432 | 29542.00 |
| | | Stage (dp [=] nm) | Midpoint (dp [=] nm) | Midpoint (dp [=] m) | Diffusion Charging | Field Charging | Total Charges | Charge (C) | Particle Mobility (m/N*s) | Slip Correction | Electric Mobility (m^2/V*s) | Settling Velocity (V/m) | Ac (m) |
| | Second iteration | 100 - 200 | 144.8478891 | 1.45E-07 | 9.67 | 0.47 | 10.14 | 1.62E-18 | 8.74E+10 | 2.148239032 | 1.42E-07 | 0.0085 | 97108.48587 |
| | | 200 - 500 | 506.9676117 | 5.07E-07 | 39.42 | 5.72 | 45.15 | 7.22E-18 | 1.54E+10 | 1.33 | 1.12E-07 | 0.0067 | 123461.0651 |
| | | 500 - 1000 | 1086.359168 | 1.09E-06 | 91.75 | 26.28 | 118.03 | 1.89E-17 | 6.26E+09 | 1.15 | 1.18E-07 | 0.0071 | 116551.3509 |
| | | 1000-2500 | 2534.838059 | 2.53E-06 | 232.93 | 143.10 | 376.03 | 6.02E-17 | 2.48E+09 | 1.07 | 1.49E-07 | 0.0089 | 92370.44608 |
| | | 2500 - 5000 | 5431.79584 | 5.43E-06 | 535.47 | 657.08 | 1192.56 | 1.91E-16 | 1.12E+09 | 1.03 | 2.13E-07 | 0.0128 | 64530.80897 |
| | | 5000 - 10000 | 10863.59168 | 1.09E-05 | 1137.05 | 2628.32 | 3765.38 | 6.02E-16 | 5.51E+08 | 1.02 | 3.32E-07 | 0.0199 | 41492.2527 |
| | | Stage (dp [=] nm) | Midpoint (dp [=] nm) | Midpoint (dp [=] m) | Diffusion Charging | Field Charging | Total Charges | Charge (C) | Particle Mobility (m/N*s) | Slip Correction | Electric Mobility (m^2/V*s) | Settling Velocity (V/m) | Ac (m) |
| RH - 80% | First iteration | 100 - 200 | 110.5396 | 1.11E-07 | 3.11 | 0.24 | 3.35 | 5.36159E-19 | 1.33561E+11 | 2.504619159 | 7.161E-08 | 0.004296597 | 110385.02 |
| | | 200 - 500 | 386.8887 | 3.87E-07 | 15.05 | 2.91 | 17.96 | 2.87422E-18 | 21785788256 | 1.429891077 | 6.26172E-08 | 0.003757032 | 126237.96 |
| | | 500 - 1000 | 829.0472 | 8.29E-07 | 37.75 | 13.37 | 51.13 | 8.18017E-18 | 8536526232 | 1.200615839 | 6.98303E-08 | 0.004189817 | 113198.27 |
| | | 1000-2500 | 1934.4435 | 1.93E-06 | 102.43 | 72.80 | 175.23 | 2.80366E-17 | 3309187928 | 1.085978215 | 9.27785E-08 | 0.005566711 | 85199.33 |
| | | 2500 - 5000 | 4145.236 | 4.15E-06 | 247.18 | 334.29 | 581.46 | 9.30344E-17 | 1479080721 | 1.040123168 | 1.37605E-07 | 0.00825632 | 57444.48 |
| | | 5000 - 10000 | 8290.4721 | 8.29E-06 | 544.76 | 1337.15 | 1881.91 | 3.01105E-16 | 725276318.7 | 1.020061584 | 2.18385E-07 | 0.013103081 | 36196.07 |
| | | Stage (dp [=] nm) | Midpoint (dp [=] nm) | Midpoint (dp [=] m) | Diffusion Charging | Field Charging | Total Charges | Charge (C) | Particle Mobility (m/N*s) | Slip Correction | Electric Mobility (m^2/V*s) | Settling Velocity (V/m) | Ac (m) |
| | Second iteration | 100 - 200 | 110.5396 | 1.11E-07 | 7.12 | 0.27 | 7.39 | 1.18E-18 | 1.34E+11 | 2.504619159 | 1.58E-07 | 0.0095 | 90554.22353 |
| | | 200 - 500 | 386.8887 | 3.87E-07 | 29.17 | 3.33 | 32.50 | 5.20E-18 | 2.18E+10 | 1.43 | 1.13E-07 | 0.0068 | 126237.96 |
| | | 500 - 1000 | 829.0472 | 8.29E-07 | 68.05 | 15.31 | 83.36 | 1.33E-17 | 8.54E+09 | 1.20 | 1.14E-07 | 0.0068 | 125616.8462 |
| | | 1000-2500 | 1934.4435 | 1.93E-06 | 173.17 | 83.34 | 256.51 | 4.10E-17 | 3.31E+09 | 1.09 | 1.36E-07 | 0.0081 | 105303.7804 |
| | | 2500 - 5000 | 4145.236 | 4.15E-06 | 398.81 | 382.68 | 781.48 | 1.25E-16 | 1.48E+09 | 1.04 | 1.85E-07 | 0.0111 | 77330.5971 |
| | | 5000 - 10000 | 8290.4721 | 8.29E-06 | 848.06 | 1530.70 | 2378.76 | 3.81E-16 | 7.25E+08 | 1.02 | 2.76E-07 | 0.0166 | 51809.31836 |

Table F.3.b.1. Salt 75% calculation results for the different relative humidity conditions.

| | Salt 25% | | | | | |
|---|---|---|---|---|---|---|
| | RH 95% | | RH 90% | | RH 90% | |
| | First iteration | Second iteration | First iteration | Second iteration | First iteration | Second iteration |
| **Concentration (Ni)** | 8.22E+12 | 8.22E+12 | 1.31E+13 | 1.31E+13 | 1.28E+13 | 1.28E+13 |
| **Number of plates** | 3273.674566 | 3273.674566 | 2057.684418 | 2057.684418 | 2103.966 | 2103.966 |
| **Velocity (m/s)** | 0.076390119 | 0.076390119 | 0.121554867 | 0.121554867 | 0.118879716 | 0.118879716 |
| **t (s)** | 78.54418959 | 78.54418959 | 49.36042603 | 49.36042603 | 50.471184 | 50.471184 |
| **NiT New** | 6.5E+14 | 6.5E+14 | 6.5E+14 | 6.5E+14 | 6.5E+14 | 6.5E+14 |

Table F.3.a.2. Salt 25% updated Nit and Nit check calculations.

From these data, the following trends can be observed. First and foremost, we can observe how – across the different salt types and humidity conditions – the peak area (our limiting factor when it comes to achieving the desired efficiency) again occurs at the accumulation mode size. This size of particles will eventually determine the total number of plates required, and thus the total cost of the project. The graphs below illustrate this condition:

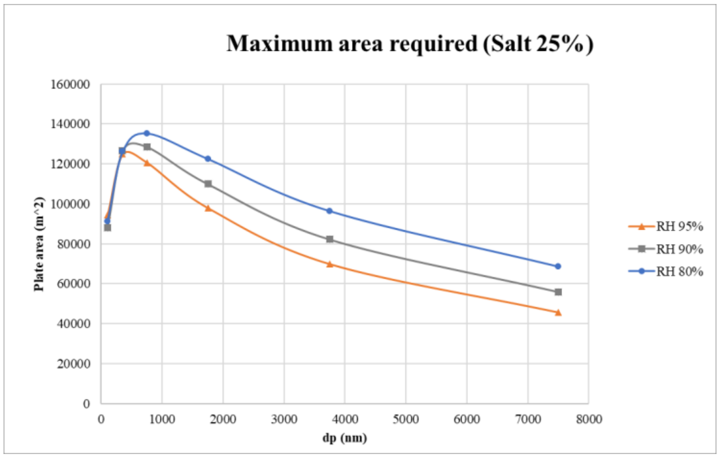


Figure F.1.a. Peak area occurring at accumulation mode for salt 25%.

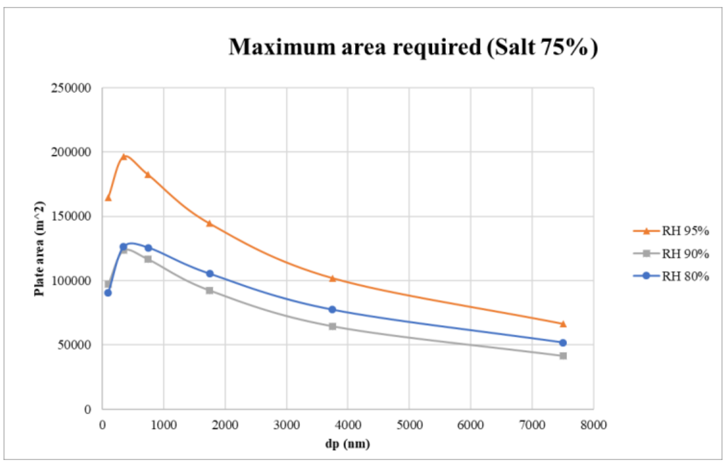


Figure F.1.a. Peak area occurring at accumulation mode for salt 25%.

Overall, the updated efficiency with the particle new concentration (Nit) appears to remain consistent across the different types of particles at different humidity values. A discrepancy occurs at Salt 75% in the 95% RH category, and this is because the particle growth and thus the plate are significantly higher compared to the other particles, which is leads to a decrease in efficiency. This phenomenon can be appreciated in Figure F.1.a., with a peak close to 200,000 m$^2$, compared to an average of (around) 120000 m$^2$. The table below summarizes the findings:

| Updated Efficiency | | | | | |
|---|---|---|---|---|---|
| RH 95% | | RH 90% | | RH 80% | |
| Salt 25% | Salt 75% | Salt 25% | Salt 75% | Salt 25% | Salt 75% |
| 0.97 | 0.90 | 0.97 | 0.96 | 0.97 | 0.97 |

Table F.4. Updated efficiencies with new Nit concentration.

Last but not least, the operation cost and the production cost can be observed in the tables below:

| Capital Cost | | | | | |
|---|---|---|---|---|---|
| RH 95% | | RH 90% | | RH 80% | |
| Salt 25% | Salt 75% | Salt 25% | Salt 75% | Salt 25% | Salt 75% |
| $ 697,154.29 | $927,085.46 | $ 709,523.99 | $ 691,952.09 | $ 733,099.47 | $ 701,716.67 |

Table F.5. Capital cost of production given by Cooper and Alley.

| Operation Cost | |
|---|---|
| Daily | Yearly |
| $80.40 | $29,344.32 |

Table F.5. Annual and Daily operational costs.

As I can be seen in Table F.4., the capital cost is in the range of ~$700,000 on average, though there is spike in the cost of an ESP that would capture Salt 75% at 95% humidity because of the increased plate area. When compared to the operation costs reported in Table F.5., it can be seen that the main cost is the capital cost, which is almost twenty-five times greater. Should the device be operated for five years, and neglecting factors such as the time-value of money, interest rates, and inflation, among others, then the net cost of year operation would be – roughly - $145,000/year (considering an average capital cost of ~$700,000).